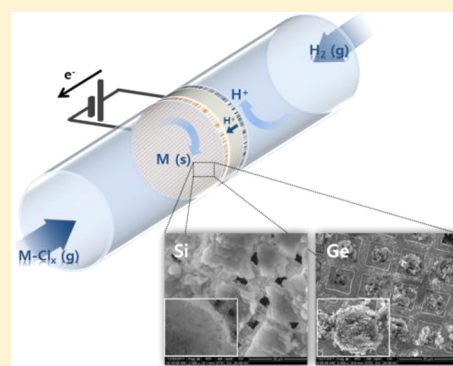# Electrochemical Vapor Deposition of Semiconductors from Gas Phase with a Solid Membrane Cell

Sung Ki Cho,[§] Fu-Ren F. Fan, and Allen J. Bard*

Center for Electrochemistry, Department of Chemistry and Biochemistry, The University of Texas at Austin, Austin, Texas 78712, United States

S *Supporting Information*

ABSTRACT: We demonstrate the feasibility of semiconductor deposition via the electrochemical reduction of gaseous precursors by the use of an anhydrous proton-conducting membrane, the solid acid $CsHSO_4$, at 165 °C. This membrane electrode assembly was operated within the oxidation of hydrogen on a porous Pt anode and the deposition of Si or Ge under bias at the cathode from chloride-based gaseous precursors; $SiCl_4$ and $GeCl_4$ in an Ar flow with a reduction potential over −1.0 V (vs RHE)

INTRODUCTION

Electrochemical deposition is one of the oldest and most widely used techniques for generating metal films. Its deposition reaction is driven by applying a potential that is more intensive and energy efficient than thermal processes, resulting in more economic production of material with good quality. Contrary to the vacuum-based technologies such as physical vapor deposition and chemical vapor deposition, electrochemical deposition is carried out in the liquid electrolyte containing ions, which could be incorporated in the deposit during deposition and become an impurity of the deposit film. The electrolyte is a major impurity source, and it is practically impossible to remove the impurity completely,[1] whereby it has a significant effect on semiconductor electrodeposition when it is applied to a photovoltaic or other device, since the impurity level in the semiconductor is critical to its physical and electrical properties.

In this study, we explore the possibility of electrochemical deposition of metals or semiconductor without using liquid electrolyte, i.e., electrochemical deposition of metal from gas phase with solid electrolyte (membrane). There are several requirements for the operation of this process: (i) Membrane itself should not be easily reduced or oxidized electrochemically; (ii) metal precursor must be in the gas phase at the operating temperature of the membrane and be reducible electrochemically; (iii) conductive ion of the membrane should be coupled with the reduction reaction of metal source to satisfy the mass balance of conductive ion in the membrane. Figure 1 shows a diagram of the reaction scheme for the reduction of a metal chloride on solid membranes.

While there has been little research on chloride-conducting membranes,[2,3] many kinds of proton-conducting membranes
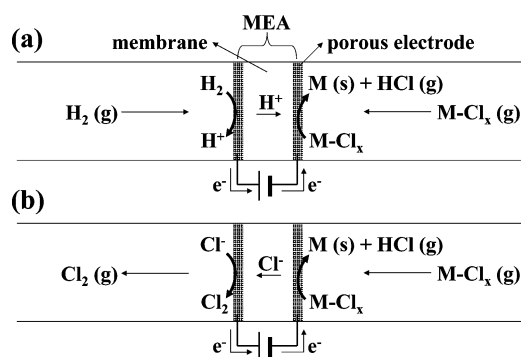

Figure 1. Conceptual diagrams of electrochemical deposition of metal from gas phase with (a) a proton-conducting membrane or (b) a chloride-conducting membrane.

such as sulfonated fluoropolymers (e.g., Nafion)[4] or poly-etheretherketone,[5] polybenzimidazole doped with phosphoric acid,[6] and perovskite-type oxides (e.g., zirconates and cerates)[7] have been developed. In many cases, water molecules play an important role in their proton conduction as they pass proton in the hydrated form of $H^+(H_2O)_n$,[8] which cannot be used for the reduction of metal chlorides, because they react chemically with water. Therefore, it is necessary to use an anhydrous pure proton conductor at a temperature well above ambient.

Solid acid, which has a structure of MH_nXO_4 {(M = K, Na, Cs), (X = S, P, Se)}, is known as a proton-conducting membrane with a high conductivity along with the structural

change, called a superprotonic transition, at a critical temperature.[8−10] Cesium hydrogen sulfate ($CsHSO_4$) is a representative of solid acid, which has a conductivity of about 10^{-2} S/cm at the temperature above its superprotonic transition point (140 °C). It is a pure proton conductor[9,10] as it has a reasonably high conductivity and a moderate operation temperature; this material is a good candidate for our purpose. In this study, we report the silicon and germanium electrodeposition from the gas phase of silicon tetrachloride and germanium chloride. To our knowledge, it is the first report of electrodeposition from a gas-phase precursor.

■ **EXPERIMENTAL SECTION**

Experimental Materials. $CsHSO_4$ was synthesized with a stoichiometric mixing of Cs_2CO_3 (Sigma-Aldrich, St. Louis, MO) and H_2SO_4 (Sigma-Aldrich, St. Louis, MO) in aqueous solution. The addition of acetone in the solution led to fast precipitation of $CsHSO_4$ particles in the solution.[9] The precipitate was filtered and dried at 60 °C in order to remove the solvent and water residues. X-ray diffractometry confirmed that powder has a monoclinic structure of $CsHSO_4$ (Figure S1a in the Supporting Information). The conductivity of $CsHSO_4$ measured by AC impedance spectroscopy (CH Instruments model 660D potentiostat, Austin, TX) showed the superprotonic transition of the conductivity near 150 °C and its conductivity was 0.01 S/cm at 160 °C (Figure S1b, see the details in the Supporting Information), which are similar to those reported in the literature.[9,10] Platinum black (Alfa Aesar, Ward Hill, MA) was used as electrode material for the reduction and oxidation of hydrogen gas. In case of the electrolysis of metal chlorides, porous metal electrodes such as gold mesh (2000, 12.7 μm spacing, SPI Supplies, Inc., West Chester, PA) or porous silver film (5 μm sized pore, SPI Supplies, Inc., West Chester, PA) were used as electrode. Contrary to metal powder-type electrode, well-defined geometry of mesh-type or porous metal film made it easier to observe the morphologies of deposits. Silicon tetrachloride ($SiCl_4$, Sigma-Aldrich, St. Louis, MO) and germanium tetrachloride ($GeCl_4$, Sigma-Aldrich, St. Louis, MO) were used as metal precursors during the electrolysis.

Fabrication of Membrane Electrode Assembly (MEA). Platinum electrodes were prepared by loading Pt black suspended in toluene (Sigma-Aldrich, St. Louis, MO) solution on carbon paper (ElectroChem, Inc., Woburn, MA) via brushing. The loading amount of Pt black was about 5 mg/cm^2. Pressing of $CsHSO_4$ powder (0.5 g) and electrodes together at 340 MPa with mechanical press resulted in a MEA pellet with thickness of 1 mm and area of about 1.32 cm^2. A single MEA has three electrodes. One (denoted as a working electrode) is a gold mesh of 0.4 × 0.3 cm^2 or a porous silver film, which is used for the reduction of metal chloride. Another (denoted as a counter electrode) is placed on the opposite side of the membrane pellet, which is a 0.6 × 0.3 cm^2 platinum electrode used for the oxidation of hydrogen gas. The other is placed next to the counter electrode, and it is a 0.4 × 0.3 cm^2 platinum electrode used as a reference electrode during the electrochemical analysis (Figure 2).
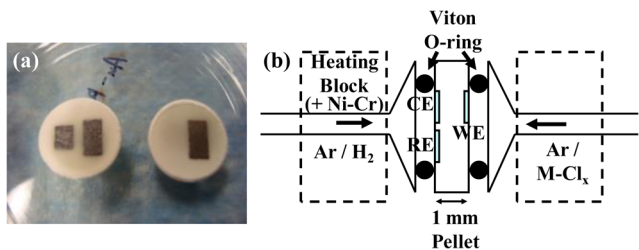

Figure 2. (a) Photograph of MEA and (b) schematic diagram of experimental setup for electrodeposition of metal from metal chloride gas.

Apparatus. Each side of the MEA was connected to a glass cell that allowed the feeding of reactant gases to the MEA which was sealed with a clamp and a Viton O-ring (see Figure 2). Electric connections to the electrodes on membrane were made by silver epoxy and copper wire. Two stainless steel heating blocks wrapped with a coiled Nichrome heating wire were placed near MEA. The reactant gas was flowed through the glass reaction chamber by passing Ar carrier gas into metal chloride solutions. The flow rate of hydrogen gas and Ar carrier gas was controlled at 200 mL/min. The operating temperature was measured with a thermocouple, placing right above the MEA, and it was controlled at 165 °C during experiments.

Electrochemical Analysis. Cyclic voltammetry and chronopotentiometry were carried out with a CHI 660D (CH Instruments model 660D potentiostat, Austin, TX). The scan rate was 100 mV/s.

Spectroscopic Analysis. After electrolysis, the MEA was immersed into benzene (Sigma-Aldrich, St. Louis, MO) to dissolve residual metal chloride left on the electrode. It was then immersed into formamide (Sigma-Aldrich, St. Louis, MO) to remove $CsHSO_4$ membrane from the electrode. The electrode was examined by scanning electron microscopy (SEM, quanta 650 FEG, FEI Company, Inc., Oregon, USA). The composition and crystallinity of deposit were characterized with an energy dispersive spectroscope (EDS, XFlash Detector 5010, Bruker, WI, USA), X-ray photoelectron spectroscope (Kratos XPS, Kratos Analytical Ltd., UK) using a monochromatic Al X-ray source, and X-ray diffractometer (D8 ADVANCE, Bruker, WI, USA) using a Cu Kα radiation source. Gas chromatography (GC, GC-2014, Shimadzu Scientific) with a thermal conductivity detector was used to analyze the gas after electrolysis. The gas product was collected in the connected glassware with all gas flow lines closed and then sampled using a syringe and was transferred to the GC instrument.

■ **RESULTS AND DISCUSSION**

Cyclic Voltammetry on $CsHSO_4$ Membrane. Before arraying out electrodeposition experiments, a study of the $I−V$ behavior of the cell and hydrogen evolution at the cathode was carried out. A few studies have discussed $I−V$ behavior on $CsHSO_4$ or CsH_2PO_4.[11−13] Since H^+ is the conducting ion in $CsHSO_4$, its continuous supply is required for sustainable current flow through the membrane. This can be achieved by hydrogen oxidation at the anode. At the same time, a reduction reaction occurs at the cathode on the other side of the membrane with hydrogen evolution as the most probable reaction in the absence of other reactant gases such as O_2, as it is not easy to reduce Cs^+ or SO_4^{2-}. Therefore, the flowing of hydrogen over the counter electrode under a positive potential bias leads to the oxidation of hydrogen, while proton reduction would occur on the working electrode. Since the reference electrode herein is placed on the same side of the membrane with the counter electrode, the reference electrode could be regarded as a reversible hydrogen electrode (RHE) as Pt electrode is in equilibrium with H_2 gas and H^+ ions inside HSO_4^{2-}. Therefore, proton reduction on the working electrode (cathode) should start at near 0 V vs the reference electrode, if the ohmic drop through the membrane is small. Figure 3 shows a cyclic voltammogram (CV) under H_2 flow over the counter electrode and Ar flow over the working electrode. The CV without hydrogen gas flow is discussed in Supporting Information (Figure S2). As expected, a large reduction current was seen near 0 V on the Pt working electrode and a change in the electrode material to a Au mesh or a porous Ag film shifted the potential of the reduction current negatively because of higher hydrogen overpotential (Figure 3a). On the counter electrode, the oxidation current with H_2 gas flow increased with an increase in H_2 partial pressure (Figure 3b). The hydrogen oxidation and evolution reactions were more clearly observed by monitoring the current with increasing bias voltage between
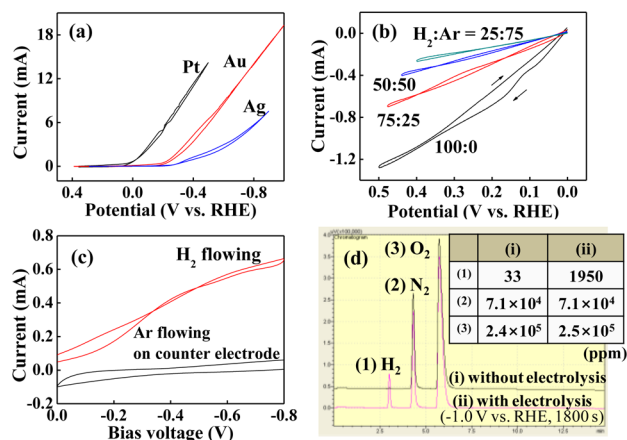
Figure 3. CVs on CsHSO$_4$ membrane with applying (a) cathode negative potentials and (b) anode positive potentials (in the presence of H$_2$ flow) with respect to reference electrode. (c) Current vs cell voltage (anode−cathode) for Pt electrodes. (d) Gas chromatogram with and without electrolysis.

working and counter electrodes (two electrodes system which is more commonly used in solid membrane electrolysis). Figure 3c shows the current developed with voltage applied between working and counter electrodes, whereas only relatively small current was observed when no hydrogen gas flowed. The proton reduction on the working electrode was verified with GC analysis by detecting H$_2$ after electrolysis (Figure 3d) in the cathode compartment. After electrolysis at −1.0 V vs RHE for 1800 s (total charge ~3.1 C), 1950 ppm of H$_2$ was detected in the Ar-filled cell on the working electrode side (total volume: 150 mL). This corresponds to 1.3 × 10^{-5} mol which is reasonably close to the theoretical value (1.6 × 10^{-5} mol). Although a small amount of air in the syringe tip as well as collected gas were introduced into GC during the injection of gas, it can be considered as a reference level because the concentrations of N$_2$ and O$_2$ were about the same as the GC analyses.

Reduction of Semiconductor Chlorides on CsHSO$_4$ Membrane. As mentioned above, the choice of metal precursor is closely connected to the electrochemical vapor deposition system. For example, studies utilized a plasma discharge for the generation of charged metal ions for metal film deposition.[14,15] In this study, metal chloride precursors were used as shown in the reaction scheme (Figure 1). Metal and semiconductor chlorides are good reactant candidates for their reduction to the element because chloride ion is a good leaving group when they are reduced electrochemically. In addition, the metal chlorides studied are volatile even at room temperature and stay in the gas phase at the operating temperature of the CsHSO$_4$ membrane. Table 1 shows the values of Gibbs free energies and relevant potentials for the

Table 1. Gibbs Free Energies and Relevant Potentials for the Reduction of Various Kinds of Chlorides

reactions ($a = 1$, $p = 1$ atm)	ΔG (kJ/mol) 25 °C	ΔG (kJ/mol) 165 °C	ΔE (V) 25 °C	ΔE (V) 165 °C
SnCl$_4$ + 4H$^+$ + 4e$^-$ → Sn + 4HCl	51.0		−0.13	
TiCl$_4$ + 4H$^+$ + 4e$^-$ → Ti + 4HCl	345.1	321.5	−0.89	−0.83
GeCl$_4$ + 4H$^+$ + 4e$^-$ → Ge + 4HCl	76.1		−0.20	
SiCl$_4$ + 4H$^+$ + 4e$^-$ → Si + 4HCl	238.6	215.7	−0.62	−0.56

reduction of various kinds of metal chlorides. The reduction reaction of the metal chlorides listed requires a negative potential bias, and consequently it needs to compete with proton reduction on CsHSO$_4$, whereby the current efficiency for the reduction of metal chloride becomes inevitably low. For this reason, working electrode materials with higher hydrogen overpotential relative to Pt are required to decrease proton reduction. At the same time, a mesh-type or porous electrode structure was used for the formation of a three-phase (i.e., electrode/membrane/reactant) boundary. We examined various materials (Figure S3) and selected an Au mesh or porous Ag cathodes in consideration of the hydrogen overpotential and chemical stability. As SiCl$_4$ and GeCl$_4$ are common metal precursors used for silicon and germanium electrodepositions in nonaqueous solution,[16−18] they were used in the present studies.

Because of competition with proton reduction, I−V scans do not exhibit a significant difference with the flow of the chloride gases (Figure S4) compared to the results in their absence. However, the electrode surface changed after electrolysis with chloride gas. Figure 4 shows the surface of Au mesh and porous
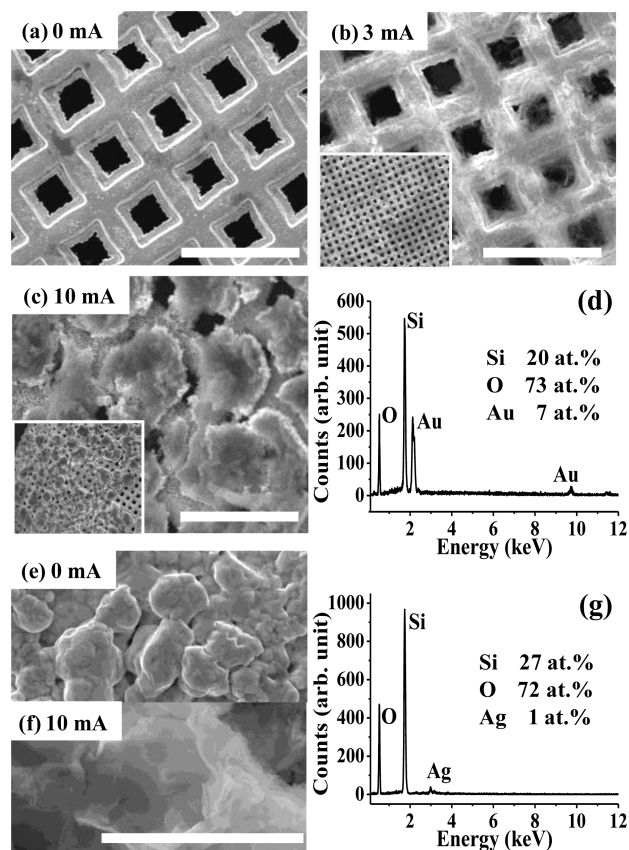

Figure 4. SEM images of (a−c) gold mesh and (e,f) porous silver film after electrolysis with various reduction current for 1500 s under SiCl$_4$ gas flow and (d,g) the EDS spectra. The scale of the white bars is 30 μm.

Ag film after electrolysis with SiCl$_4$ gas flow. All surfaces shown in the SEM images are the cathodic sides that were contacted to the CsHSO$_4$ membrane during the electrolysis, after the membrane was removed by dipping in formamide after electrolysis. Figure 4a,e shows the surfaces of Au mesh and porous Ag film without potential bias during SiCl$_4$ flow, indicating that the chemical reaction did not occur between

$CsHSO_4$ and $SiCl_4$. After the electrolysis at a constant reduction current, Si deposits were found on the electrodes, and their amount increased with the reduction current applied. As mentioned above, little difference in CV (Figure S4) indicates the low current efficiency for the deposition, and unfortunately, it was not straightforward to estimate the deposit amount due to irregular deposit shape.

Another route to the reduction of $SiCl_4$ is through chemical reaction with electrogenerated hydrogen gas. However, this chemical reaction usually occurs at very high temperature (>800 °C),[19] and therefore, it is more reasonable that $SiCl_4$ was reduced directly electrochemically. Sometimes part of electrode came off the membrane after the electrolysis, which might be due to the deposit formation on the membrane surface. Figure 5 shows the time-evolved growth of the silicon deposit, which
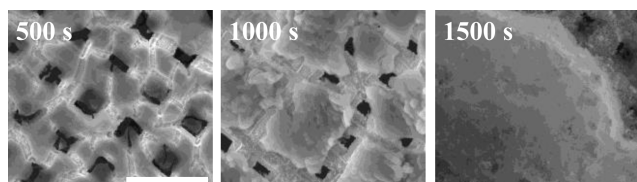

Figure 5. SEM images of time-evolved growth of silicon by electrolysis (10 mA) on Au mesh under $SiCl_4$ gas flow. The scale of the white bars is 30 μm.

grew toward the membrane, since the reaction presumably occurs only at the three-phase boundary. The growth of deposit toward membrane forms a new electrode, which includes the deposit, contacted consistently to the membrane, and the reactant gas, $SiCl_4$ reaches the boundary through the deposit, as the deposit should be porous. This leads to the formation of a new three-phase boundary and the continuous growth of silicon. The growth of deposit, therefore, might generate and widen the gap between electrode and membrane. The silicon deposit was amorphous and porous, and its morphology was similar to the silicon deposit from electrodeposition in nonaqueous solution.[16] EDS analysis showed that silicon deposit is in oxide form. Since the color change of the Si deposit-covered electrode was observed during the electrode transfer to the SEM chamber, we speculate that fast oxidation of silicon may occur even for short time exposure to air, as many amorphous and porous silicon deposits experienced.[16] XPS analysis showed an Si^{4+} peak which corresponds to the silicon oxide, and very weak Si^0 peak was detected after Ar^+ sputtering (10 min), indicating that the silicon deposit is extremely easy to oxidize because of its porous structure (Figure S5). However, impurities such as Cl, Cs, and S were not detected by EDS, which is also confirmed by XPS analysis. As the impurity whose level beyond the detection limit of XPS (0.1 at. %) is critical to semiconductor properties, it is necessary for impurities to be analyzed precisely, and it will be addressed in future studies.

The electrolysis with $GeCl_4$ also generated Ge deposit on the surface, and the result was closer to expectations (Figure 6). Although the chemical reaction between $CsHSO_4$ membrane and $GeCl_4$ was not observed (inset in Figure 6a), applying of reduction current through the electrodes resulted in Ge deposit (Figure 6a). A strong Ge peak was observed on the EDS spectrum (Figure 6b), indicating that the deposit mostly consisted of elemental Ge. Interestingly, the Ge deposit grew as a globular form, while the silicon deposit had a more planar
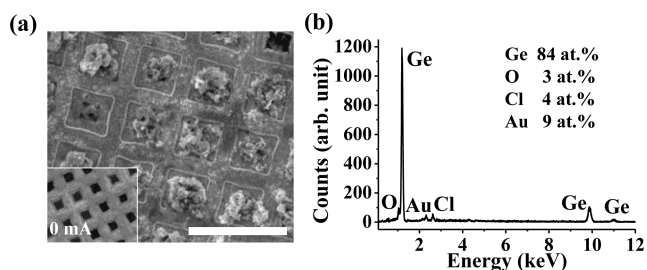

Figure 6. (a) SEM images of gold mesh after electrolysis with reduction current of 10 mA for 1000 s under $GeCl_4$ gas flow and (b) its EDS spectrum. The scales of the white bars are 30 μm.

shape. This might be interpreted in terms of the difference in the resistivity between Si and Ge deposits. As the deposit grows, the electron required for the continuous reduction and growth passes through the underlying deposit layer, whereby the resistivity of deposit layer has an effect on the electron transfer, especially when the deposit is not very conductive.

Intrinsic silicon has a relatively high resistivity (10^4 to 10^5 Ω·cm), and it is known that the silicon deposit passivates the electrode surface in electrochemistry,[16] so that it is more favorable for silicon to grow on adjacent electrode surface rather than on the top of the resistive silicon deposit. Germanium, on the other hand, is more conductive (<10^2 Ω·cm), whereby the electron might be transferred well through the deposit to top surface and accordingly a deposit grows three-dimensionally. There is a small peak of Cl in the EDS spectrum. We speculate that the small amount of Cl corresponds to the existence of $GeCl_2$. As the generation of $GeCl_2$ was observed during the electrochemical reduction of $GeCl_4$ to Ge in nonaqueous solution,[17,18] it is possible that small amount of $GeCl_2$ is left inside the deposit due to the incomplete reduction. The oxygen peak would indicate the native oxide on the surface, but it is much smaller than that of silicon deposit. Figure 7 shows the continuous growth of Ge with the electrolysis time.
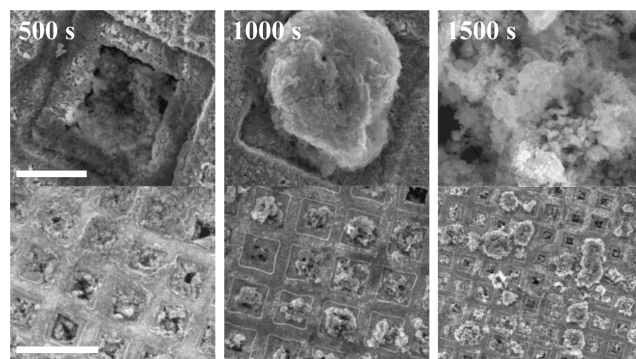

Figure 7. SEM images of time-evolved growth of germanium by electrolysis on Au mesh under $GeCl_4$ gas flow. The scales of the white bars is 5 μm (top row) and 30 μm (bottom row), respectively.

XPS results were consistent with EDS (Figure 8). Germanium in the form of oxides (GeO_2, GeO) was detected on the surface, whereas elemental state of Ge was found after 5 min of Ar^+ sputtering, which corresponds to about 50 nm etching, and the atomic concentration ratio of Ge to O increased with the sputtering time. As compared to silicon deposits, the globular shape of Ge deposit might help to
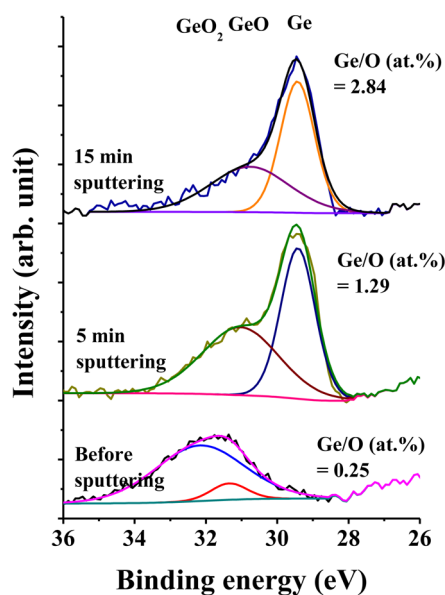
Figure 8. X-ray photoelectron spectrum of Ge 3d of germanium deposit which was deposited on gold mesh (10 mA, 1500 s).

prevent the complete oxidation during the exposure to ambient condition. The existence of metallic germanium is a strong evidence of the reduction of metal chloride in gas phase. From XRD analysis, the Ge deposit was found to be amorphous (Figure S6).

CONCLUSIONS

In summary, electrochemical semiconductor deposition from gas-phase precursors has been demonstrated by using a proton-conducting membrane. $CsHSO_4$ proton conduction was verified by hydrogen generation with negative potential bias and hydrogen oxidation with positive potential bias. Silicon and germanium chlorides can be reduced electrochemically on the $CsHSO_4$ surface, yielding amorphous silicon and germanium deposits. The properties of the membrane probably have significant influence on the deposit properties, and therefore, it is necessary to explore the electrochemical reduction of metal precursors on other membranes such as perovskite oxides or chloride-conducting membranes. The reduction of other metal precursors should also be possible, and more noble metals, like Pt, should be possible to deposit on the membrane with a carbon layer as contact. We envision such studies in future work.

ASSOCIATED CONTENT

Ⓢ Supporting Information

Additional experimental data figures. The Supporting Information is available free of charge on the ACS Publications website at DOI: 10.1021/jacs.5b02878.

AUTHOR INFORMATION

Corresponding Author
*ajbard@cm.utexas.edu

Present Address
§School of Energy and Integrated Materials Engineering, Department of Energy and Chemical Engineering, Kumoh National Institute of Technology, 61 Daehak-ro, Gumi-si, Gyeongsangbuk-do 730−701, Republic of Korea.

REFERENCES

(1) Schlesinger, M.; Paunovic, M. In *Modern Electroplating*, 4th ed.; John Wiley & Sons, Inc.: Hoboken, NJ, 2000; pp36.

(2) Yamada, K.; Isobe, K.; Tsuyama, E.; Okuda, T.; Furukawa, Y. *Solid State Ionics* **1995**, *79*, 152−157.

(3) Murin, I. V.; Glumov, O. V.; Mel'nikova, N. A. *Russ. J. Electrochem.* **2009**, *45*, 411−416.

(4) Mauritz, K. A.; Moore, R. B. *Chem. Rev.* **2004**, *104*, 4535−4586.

(5) Kreuer, K. D. *J. Membr. Sci.* **2001**, *185*, 29−39.

(6) Ma, Y.-L.; Wainright, J. S.; Litt, M. H.; Savinell, R. F. *J. Electrochem. Soc.* **2004**, *151*, A8−A16.

(7) Kreuer, K. D. *Annu. Rev. Mater. Res.* **2003**, *33*, 333−359.

(8) Devanathan, R. *Energy Environ. Sci.* **2008**, *1*, 101−119.

(9) Haile, S. M.; Boysen, D. A.; Chisholm, C. R. I.; Merle, R. B. *Nature* **2001**, *410*, 910−913.

(10) Chisholm, C. R. I.; Jang, Y. H.; Haile, S. M.; Goddard, W. A., III *Phys. Rev. B* **2005**, *72*, 134103 (1−20).

(11) Kuzuoka, Y.; Wen, C.-J.; Otomo, J.; Ogura, M.; Kobayashi, T.; Takahashi, H. *Solid State Ionics* **2004**, *175*, 507−510.

(12) Louie, M. W.; Hightower, A.; Haile, S. M. *ACS Nano* **2010**, *4*, 2811−2821.

(13) Shimada, I.; Oshima, Y.; Otomo, J. *J. Electrochem. Soc.* **2011**, *158*, B369−B375.

(14) Cole, J. J.; Lin, E.-C.; Barry, C. R.; Jacobs, H. O. *Small* **2010**, *6*, 1117−1124.

(15) Barry, C. R.; Cole, J. J.; Jacobs, H. O. *Nano Lett.* **2010**, *10*, 4494−4500.

(16) Munisamy, T.; Bard, A. J. *Electrochim. Acta* **2010**, *55*, 3797−3803.

(17) Meng, X.; Al-Salman, R.; Zhao, J.; Borissenko, N.; Li, Y.; Endres, F. *Angew. Chem., Int. Ed.* **2009**, *48*, 2703−2707.

(18) Al-Salman, R.; Abedin, S. Z. E.; Endres, F. *Phys. Chem. Chem. Phys.* **2008**, *10*, 4650−4657.

(19) Eversteyn, C. *Philips Res. Rep.* **1974**, *29*, 45−66.